Environmental and anthropogenic drivers of surface urban heat island intensity
A case-study in the Yangtze River Delta, China

Wang, Zian; Meng, Qingyan; Allam, Mona; Hu, Die; Zhang, Linlin; Menenti, Massimo

DOI
10.1016/j.ecolind.2021.107845

Publication date
2021

Document Version
Final published version

Published in
Ecological Indicators

Ecological Indicators 128 (2021) 107845

Contents lists available at ScienceDirect

Ecological Indicators

journal homepage: www.elsevier.com/locate/ecolind

Environmental and anthropogenic drivers of surface urban heat island intensity: A case-study in the Yangtze River Delta, China

Zian Wang [a,b,c], Qingyan Meng [a,c,e,*], Mona Allam [a,d], Die Hu [a,c,e], Linlin Zhang [a,c,e], Massimo Menenti [a,f]

[a] Aerospace Information Research Institute, Chinese Academy of Sciences, Beijing 100101, China
[b] University of Chinese Academy of Sciences, Beijing 101400, China
[c] Sanya Institute of Remote Sensing, Sanya 572029, China
[d] Environment & Climate Changes Research Institute, National Water Research Center, El Qanater El khairiya 13621/5, Egypt
[e] Hainan Research Institute of Chinese Academy of Sciences, Sanya 572029, China
[f] Geosciences and Remote Sensing Department, Delft University of Technology, Stevinweg 12628 CN, Delft, the Netherlands

ARTICLE INFO

Keywords:
Surface urban heat island
Land surface temperature
Boosted regression trees
Yangtze River Delta

ABSTRACT

Nowadays urban climate is a global problem and many studies focused on understanding the relation between urban climate the built-up space using radiometric observations of the land surface temperature to estimate and monitor the surface urban heat island intensity (SUHIs). In this study MODIS land surface temperature (LST) data were used. The Yangtze River Delta Urban Agglomeration (YRDUA), eastern China, was selected as an example to study SUHI and multiple influencing factors in 16 big cities. Anthropogenic factors are considered the most important ones in determining SUHI, while natural factors remain influential. By using stratified random sampling (SRS), 78,085 random points were selected within the 16 cities. Nine influencing factors were selected in this study: distance from building (BD), distance from the main roads (RD), distance from water (WD), digital elevation model product (DEM), gross domestic product (GDP), normalized difference vegetation index product (NDVI), nighttime lighting intensity (NTI), population (POP) and impervious surface area data (%ISA). The SUHI intensity was extracted at each random point as well as the values of the influencing factors, NDVI, DEM, ISA, POP, NTI and GDP. For BD, WD and RD, random points were selected from the water, building and main roads using the near tool in ArcGIS to measure these distances. Boosted regression tree (BRT) model was applied to capture the contributions of the above factors to SUHI. We also applied a different procedure to evaluate the relative influence of Land Use and Land Cover (LULC). The relative influence refers to the contribution of each factor to determine SUHI. The influencing factors were ranked on the basis of the relative influence on SUHI. The results showed that (1) higher SUHI intensity was recorded in Shanghai, Jiaxing and Nanjing cities respectively, while Hangzhou recorded the lowest SUHI. (2) Anthropogenic drivers have slightly higher relative influence on SUHI than natural drivers, i.e. 51.29% and 48.71% respectively. The influence of all drivers on SUHI from high to low is NTI (27.62%), ISA (24.38%), NDVI (12.11%), GDP (7.95%), DEM (7.29%), POP (6.37%), BD (5.33%), WD (4.93%), RD (4.02%). (3) The variation in the socioeconomic level lead to different spatial patterns of different influence factors, further indicating that the overall mean SUHI intensity is affected by the development of the city.

1. Introduction

According to the World Urbanization, 54% of the world's population lives in urban areas, and this percentage is expected to reach 66% by 2050 (United Nations, 2014). Impervious surfaces, such as cement, asphalt and concrete have gradually replaced the natural land surfaces

Abbreviation List: LST, land surface temperature; UHI, urban heat island; SUHI, surface urban heat islands; YRDUA, Yangtze River Delta Urban Agglomeration; DEM, digital elevation model; NDVI, normalized difference vegetation index; ISA, impervious surface area; NTI, nighttime lighting intensity; LULC, land use and land cover change; POP, population; GDP, gross domestic product RD/BD/WD, distance from the major roads/building/water; BRT, boosted regression trees.

* Corresponding author at: Aerospace Information Research Institute, Chinese Academy of Sciences, Beijing 100101, China.
E-mail address: mengqy@radi.ac.cn (Q. Meng).

https://doi.org/10.1016/j.ecolind.2021.107845
Received 25 November 2020; Received in revised form 19 April 2021; Accepted 24 May 2021
Available online 1 June 2021

as a result of the accelerating urbanization process (Lo et al., 1997). These changes affect many things including the energy exchange between the land surface and the atmosphere. Urbanization also leads to changes in the climatic system, threatens biodiversity and affects ecosystem productivity through energy imbalance and loss of carbon storage (Cui et al., 2012; Seto et al., 2012). The relative increase in the temperature of a city relative to its surroundings is called the "urban heat island (UHI) effect" (Martilli et al., 2020; Oke, 1995).

UHI affects all kinds of living organisms in the urban areas (Zhang et al., 2013), affects the health of urban residents and increases air pollution (Zhang et al., 2019)(Li et al., 2017a). Therefore, it is important to understand which factors determine UHI and what is their relative weight in order to develop proper urban policies in the future (Hu et al., 2020b), and to reduce the expected negative impacts of urban heat (Martilli et al., 2020). Anthropogenic heat, which consists of the heat discharged from industrial plants, space heating, human metabolism and vehicle exhausts, is a major contributor to UHI. In cities, this heat usually contributes 15–50 W/m^2 to the local heat balance (Sobrino et al., 2008).

The UHI can be calculated by air temperature, while the surface urban heat island (SUHI) is calculated with observations of the land surface temperature (Streutker, 2003; Li et al., 2017b). Air temperature is measured at weather stations while land surface temperature (LST) is retrieved from airborne and satellite data. This study focuses on estimating SUHI and to evaluate the multiple properties of urban areas which might influence SUHI in 16 big cities. The weight of each influencing factor and its effect on the spatial heterogeneity of SUHI was evaluated.

Several previous studies focus on SUHI, e.g. Ayanlade (2016), Clinton and Gong 2013), Lu et al. (2014) and Weng (2009). Factors affecting SUHI can be divided into: (1) Surface biophysical factors which include LULC, NDVI (normalized difference vegetation index) (Liu et al., 2016; Zhou et al., 2014c), NDBI (normalized difference built-up index) were widely used in SUHI studies (Chen et al., 2006; Liu and Zhang, 2011; Du et al., 2016c) (2) Socio-economic factors include population density (Huang and Cadenasso, 2016; Kotharkar and Surawar, 2016; Weng et al., 2008), distance from the building (BD), the main roads (RD) and the water (WD) (Feng et al., 2019). Also including gross domestic product (GDP), which is an indicator to the economic level in the city (Cui et al., 2016), and nighttime light data (nW cm^{-2} Sr^{-1}), it is an indicator of the human density in a specific area (Peng et al., 2012). ISA was also studied here, which it is defined by artificial structures that prevent infiltration of water into the soil (Bounoua et al., 2018; Gong et al., 2019).

Some of the previous studies applied one influencing factor at the time in a regression analysis (Pearson correlation analysis, ordinary least-squares regression analysis, geographically weighted regression (GWR) analysis), and compared individual effects on SUHI on the basis of the coefficient of regression (R^2). SUHI is usually affected by multiple factors, therefore, the strength of coefficient of regression (R^2) for a single-factor cannot accurately explain observed SUHI. Most previous studies focused on an individual factor (Imhoff et al., 2010; Jusuf et al., 2007; Oke, 1973; Tan and Li, 2015), while a few studies focused on the effects of multiple factors on SUHI (Coseo and Larsen, 2014; Peng et al., 2012).

Currently most stepwise regression methods are used in SUHI studies. Even though this method can generate an accurate model to explain the observed SUHI, it is difficult to estimate the contribution of all influencing factors. In brief, a small number of researches focused on detecting the ranking of the influencing factors on SUHI.

The study was carried out in the Yangtze River Delta Urban Agglomeration (YRDUA), China. This study aimed to assess SUHI and the influencing factors using boosted regression trees (BRT). The main purposes of the study were: (1) investigate the effects of influencing factors on the SUHI and to detect the prevailing factors; (2) compare the effects of these factors on SUHI in the 16 selected cities.

The research questions can be summarized as follows:

(1) What is the pattern of SUHI in YRDUA?

(2) What are the relations between influencing factors and SUHI on agglomeration scale and what is the contribution rate of each factor?

(3) Is the relative effect of influencing factors on SUHI r similar in different cities?

(4) Is the BRT model more effective than other statistical methods?

2. Material and methods

2.1. Study area

The Yangtze River Delta is located in the east of China, adjacent to the East China Sea (118°30 '00 "E-123°00′ 00″ E, 28°00 '00 "N-33°30′ 00″ N). Its area is 9.96 × 10^4 km^2, and the total urban area is 4.19 × 10^{3}km^2 (Hu et al., 2009). In this study, YRDUA refers to an area consisting of a core city (Shanghai), two sub-core cities (Nanjing and Hangzhou) and 13 other prefecture-level cities in southeastern Jiangsu province and northern Zhejiang province. It is surrounded to the east by Shanghai, to the south by Taizhou and to the west by Hangzhou (Fig. 1). The topography of YRDUA is largely composed of plains and various landforms like hills and mountains. YRDUA belongs to the subtropical monsoon climate, the average annual precipitation and temperature are 804 to 2057 mm and 9.3 to 17.3 °C respectively (Yang et al., 2017). This region is regarded as one of the most developed ones in China, and most industries are concentrated in this area (Huang and Lu, 2015). The urban agglomeration of the Yangtze River Delta region is one of the important six urban areas in the world, because it plays an important role in China's economic and social development (Gu, 2011; Tian, 2011). The YRDUA accounts for a quarter of the country gross domestic product (GDP) (Zhou et al., 2018). Rapid urbanization led to the decrease of land resources and environmental quality (Sun et al., 2019).

In 2015, China's GDP reached 1,087.7 billion US dollars (Gao et al., 2019). At the same time, the region is one of the highest densities on the world, with 82.3 million people in 2015, 53.6 million of them living in the urban areas (Zhou et al., 2018). So for the above mentioned reasons, YRDUA was selected as our study area Rapid urbanization has accelerated surface warming of YRDUA (Du et al., 2016b; Yang et al., 2011).

2.2. Data description and preprocessing

LST data were derived from MOD11A2 data products available at the Geospatial Data Cloud (http://www.gscloud.cn/). The 2015 data were used to study the SUHI pattern and drivers of SUHI in the YRD.

Nighttime light satellite images have been widely used to detect, estimate, and monitor socioeconomic dynamics (Bennett and Smith, 2017). With updated remote sensing data and the development of technology, nighttime light satellite data with higher resolution have become available. NPP-VIIRS data (spatial resolution: 750 m) may be a powerful tool for modeling socioeconomic indicators (Shi et al., 2014). NTL VIIRS data not only detect urban population, but also reflect the level of urbanization in detail (Chen et al., 2015). The sensor can also detect the artificial light from the earth's surface and have been used to study social-economic activities (Elvidge et al., 1997). In this study, the Suomi-NPP-VIIRS data (https://ngdc.noaa.gov/) was used to assess nighttime lighting intensity (NTI). Most potential driving factors requiring data on roads, buildings and waters, were evaluated using data extracted from Open Street Map (OSM, https://www.openstreetmap.org/). The GDP and POP data were extracted from the Resource and Environment Science and Data Center (http://www.resdc.cn/).

The impervious surface products are the ones described by Gong et al. (2019). The DEM and NDVI products are derived from geospatial data cloud (http://www.gscloud.cn). The original LULC mapped 21 classes, which were aggregated into six classes for the purpose of our study: (1) Built-up area, including buildings, streets and other artificial surfaces; (2) Grassland (including natural grassland and artificial

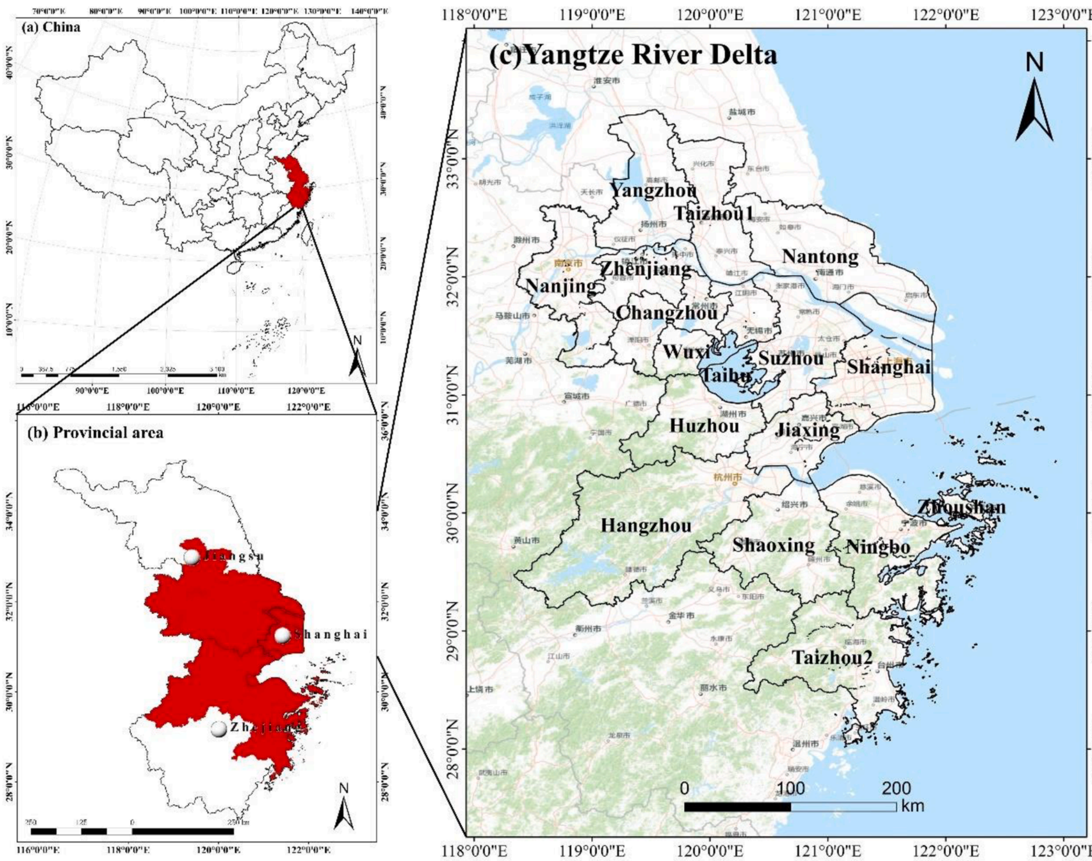

Fig. 1. Location of the study area. (a) China. (b) Provincial area of Jiangsu, Zhejiang and Shanghai. (c) Yangtze River Delta.

grassland); (3) Water body (including lakes, reservoirs and rivers); (4) Forest land (including land with natural forests, plantations and urban trees); (5) Farmland land (including paddy fields and dry land); (6) Unutilized land (including bare land and the leveled unused land).

The influence of the data spatial resolution on LST should not be underestimated, therefore, all data for factor calculations were resampled to a 1000 m × 1000 m resolution within the study area as delineated with ArcGIS 10.2. The potential driving factors were selected based on the literature review and available data (Table 1).

2.3. Rural area

We selected 16 cities for our study (Fig. 1). The retrieved LST was improved by correcting for noise caused by cloud contamination, topographic differences and zenith angle changes (Wan, 2008). The validation of the MODIS LST data against the in situ LST data indicate that the accuracy of the MODIS LST data (Du et al., 2016a; Wan, 2008).

The choice of an appropriate and stable rural reference is most important in studies on SUHI. For this purpose, rural areas can be identified according to the following criteria (Liu et al., 2018):

1. Flat fields on the same altitude as the city: The difference in elevation between the rural point of comparison and the urban region in question should be ≤ 50 m on a level, horizontal surface in order to ensure that the results of the assessment are not affected by temperature differences due to terrain exposure and elevation.

2. Areas with a nighttime light intensity value ≤ 1. By using nighttime light intensity, one can identify areas that are virtually unaffected by human activity, including rural backgrounds where the heat island effect is not present. Although the outskirts of the cities are primarily composed of farmlands and vegetation, they are also affected to a relatively large degree by urbanization, and therefore are not suitable for use as a rural reference in a study on SUHI. Therefore, only areas where the nighttime light intensity is ≤ 1 have been chosen as the rural reference for this study.

3. Areas where the maximum annual NDVI value is ≥ 0.7. By using this index, one can identify areas that are purely composed of highly concentrated vegetation and which do not include bodies of water and exclude many areas of low vegetation coverage in the outskirts of the cities, such as rural villages or satellite towns. The index can be obtained using the annual maximum NDVI image for 2015.

2.4. Surface urban heat island intensity (SUHI) calculation

The SUHI intensity has been estimated as the LST difference between urban and rural areas, with the aid of ancillary information, as LULC and ISA (Deilami et al., 2018). SUHI intensity has been calculated in this study as follows: 1. delineated the rural areas as discussed in section 3.1. 2. Delineated the rural area using Arcgis 10.2. 3. From LST image the rural area was clipped to get the LST for rural areas.4. We calculated the mean LST for rural area. 5. SUHI was then calculated by subtracting the mean LST of rural area from LST (Oke, 1982; Schwarz et al., 2011; Zhou et al., 2014a):

$$\Delta LST^{i} = LST^{i}_{urban} - LST_{rural} \tag{1}$$

Where LST^{i}_{urban} is the urbanLST , i = random points, i = 1,…, N. N = 3297 in Changzhou, N = 12128 in Hangzhou, N = 4646 in Huzhou, N = 2940 in Jiaxing, N = 4941 in Nanjing, N = 6573 in Nantong, N = 5835 in Ningbo, N = 3655 in Shanghai, N = 5445 in Shaoxing, N = 5976 in Suzhou, N = 4511 in Taizhou1, N = 6533 in Taizhou2, N = 3422 in Wuxi, N = 5046 in Yangzhou, N = 2817 in Zhenjiang, N = 320 in Zhoushan. And LST_{rural} is the mean LST in the rural area.ΔLST^{i} represents the SUHI intensity at point i.

Table 1
The potential driving factors selected in this study.

Type	Name(ad)	Definition	Date source
Natural factors	Digital elevation model (DEM)	DEM is digital elevation model, it characterizes the topographical variation (elevation) of the study area (Wang et al., 2018).	http://www.gscloud.cn
	Normalized difference vegetation index (NDVI)	NDVI is normalized difference vegetation index, it reflects vegetation coverage and intensity (Hu et al., 2020b).	http://www.gscloud.cn
	Impervious surface area (ISA)	ISA is artificial structure that prevents infiltration of water into the soil, includes roofs, paved surfaces (Bounoua et al., 2018; Gong et al., 2019).	(Gong et al., 2019)
	Distance from the water (WD)	WD is one of the distance-based proximity factors, it is the distance from the water (Feng et al., 2019).	http://www.openstreetmap.org
	Land use and land cover changes (LULC)	LULC, It has direct relation with the global warming as well as with modification of local climate and environment in a microclimate region (Guo et al., 2018; Pramanik and Punia, 2019).	http://www.resdc.cn
Anthropogenic factors	Gross domestic product (GDP)	GDP is gross domestic product. It reflect the level of economy in the city (Cui et al., 2016).	http://www.resdc.cn
	Population (POP)	POP is considered an indicators of anthropogenic heat, which reflects the spatial distribution of residents (Du et al., 2016b).	http://www.resdc.cn
	Nighttime light product (NTL)	NTI is nighttime lighting intensity, it is indicator to the density of human. Low nighttime lighting intensity is directly generated by agricultural activities, especially for undeveloped regions where slow urbanization occurs (Peng et al., 2012).	https://ngdc.noaa.gov
	Distance from the major roads (RD)	RD it is the distance from main roads to the center. It is a measure of urban density: long RD means low urban density (Feng et al., 2019).	http://www.openstreetmap.org
	Distance from the building (BD)	BD is one of the distance-based proximity factors, it is the distance from the main building. Large BD means far from building (Feng et al., 2019).	http://www.openstreetmap.org

2.5. Selection of the influencing factors

The influence of the UHI effect is complex and varied, and contains a great deal of information. According to the previous results on UHI effect, the driving factors were divided into natural and anthropogenic factors. Ten potential driving factors were selected in the BRT model based on the literature review and available data.

Normalized difference vegetation index (NDVI) (Tucker et al., 1985) has been widely used to characterize vegetation coverage (Hu et al., 2020b). Previous studies have shown that SUHI is negatively correlated with NDVI (Yuan and Bauer, 2007).

Nighttime lighting intensity (NTI) is derived from nighttime light remote sensing images to represent economic development. Logarithmic conversion of the NPP-VIIRS nighttime light composite data has been used to establish a quantitative indicator, the NTI (Yu et al., 2018).

Distance to the major roads (RD), buildings (BD) were calculated from urban road and building vector data, which are commonly used as indicators of the anthropogenic heat, several studies documented the influence of the distance to roads on thermal environment (Hien et al., 2011; Wang et al., 2014).

Besides, the Yangtze River flows through Jiangsu Province, which is one of the largest rivers in North China, and there are 49 tributaries of the Yangtze River running through Jiangsu Province, with a total length of 26.2 km. Taihu Lake covers an area of 0.224 km^2 was also considered. Water-cooling islands are important for mitigating UHI effects of ultra-high heat (Du et al., 2016), therefore, distance to waters (WD) has been established as an indicator of natural factors.

With the fast-economic development and rapid population all over the world, the rate of urbanization increased and impervious surfaces replaced the natural ones (Stankowski, 1972). The GDP and population were considered as drivers of SUHI (Zhao et al., 2016).

The fractional abundance of impervious soil cover is considered the main determinant of SUHI (Zhao et al., 2016). When computing the % ISA of each pixel, the fishnet with the same resolution as the LST data was established and the fractional abundance of impervious surfaces was calculated.

Elevation of the natural surface of the Earth remains the same over a period of time and does not undergo any major change, even after urbanization (Wang et.al, 2015). The Digital Elevation Model (DEM) data with a 90-m resolution were used to characterize the elevation within the study area.

The effects of the influencing factors on SHUI are calculated as follows: 1-The calculated SUHI in section 2.4 is classified into 10 classes using ArcGIS classification tool (Jenks classification) and the area of each class was calculated; 2- By using stratified random sampling (SRS) method (Nguyen et al., 2019), 78,085 random points were selected in the whole study area, the number of random points was selected according to the area of each class. For Hangzhou, there was the largest number of random points (12128) while for Zhoushan, the numbers of random points were the lowest one, i.e. 320; 3- Each city was clipped in the SUHI map. 4- Distances from these points to main roads, buildings and waters were calculated using the near tool in ArcGIS toolbox. 5-SUHI were extracted at these points. 6- The values of NDVI, elevation, ISA, POP, GDP, NLI were also extracted at the same points. 7- All the extracted values are applied in the BRT model in R (R Development Core Team, 2006) version 2.3–1, using gbm package, then the relative influence and its contribution of each factor are calculated. 8- Each LULC class has no numerical value, thus the regression analysis cannot be done in the same way as with the other factors. Assign a number to each LULC type, then extracted at the selected random points and applied in combination with SUHI to BRT model. The results are then assigned back to the original LULC type, so the relative influence of LULC on SUHI in the 16 cities was gotten.

2.6. Boosted regression trees analysis

A machine learning statistical method called a boosted regression tree (BRT) was used to analyze the natural and anthropogenic factors in the complex urban environment. The BRT approach is fundamentally different from usual technique of using a tool to quantify the relationship between one variable and another. The BRT combines two algorithms, regression tree and boosting, in a single process (Friedman, 2002). The process iteratively splits the space defined by independent variables to construct the dependent variable model. With the increase of split number, the accuracy of the model is improved. The tree-based model uses a series of rules to identify the regions with the most uniform response to predictive variables, thus dividing the predictive variable space into multidimensional subspaces. Friedman (2002) proposes a definition of the “relative influence” of a variable (where relative influence refers to the contribution of each variable). For each of the next steps, the focus is on the residuals: changes in the model’s response that have not been explained so far. Statistical deviation is used as the loss function of the software we use (please refer to https://statisticaloddsandends.wordpress.com/2019/03/27/what-is-deviance/).

The analysis was performed using the statistical programming software R version 3.3.2 with the gbm package. In gbm, randomness is controlled by “bag fraction”, which specifies the proportion of data to be selected for each step. The default bag fraction is 0.5, which means that in each iteration, 50% of the data will be randomly selected from all the training sets without replacement. In our study, 50% of the data was used to fit our independent variable, SUHI as the first regression tree.

3. Results

3.1. Spatial pattern of SUHI

Using the MODIS LST data for the year 2015, the annual mean SUHI intensity was calculated (Fig. 2). It is clear that the SUHI is higher in the central and eastern parts of the study area including Shanghai, Suzhou and Jiaxing. In Shanghai, the SUHI intensity reaches up to 5.7 °C in downtown areas in the centre and northern part of Shanghai. Hangzhou, Ningbo and Taizhou also showed high SUHI intensity to some extent but less than Shanghai and Nanjing. One of the important reasons for this is the large vegetation areas that are spreading in these cities. Hangzhou has been named “International Garden City” by the International Federation of Park and Recreation. This confirms the important of urban vegetation in reducing SUHI.

In the YRDUA, there is a “SUHI string cluster” with Shanghai at its center and a series of cities in the northwest, including Suzhou, Wuxi and Changzhou. In the northwestern cities of Nanjing, Yangzhou and Zhenjiang (close to each other), SUHI intensity was also well known to be rather high, same as Hangzhou and Ningbo (near Hangzhou Bay). The high SUHI largely occurs in the cities surrounding Shanghai. Due to the limited land area of Shanghai, its heat island cannot spread out much. In the future, these cities are expected to expand SUHI within this

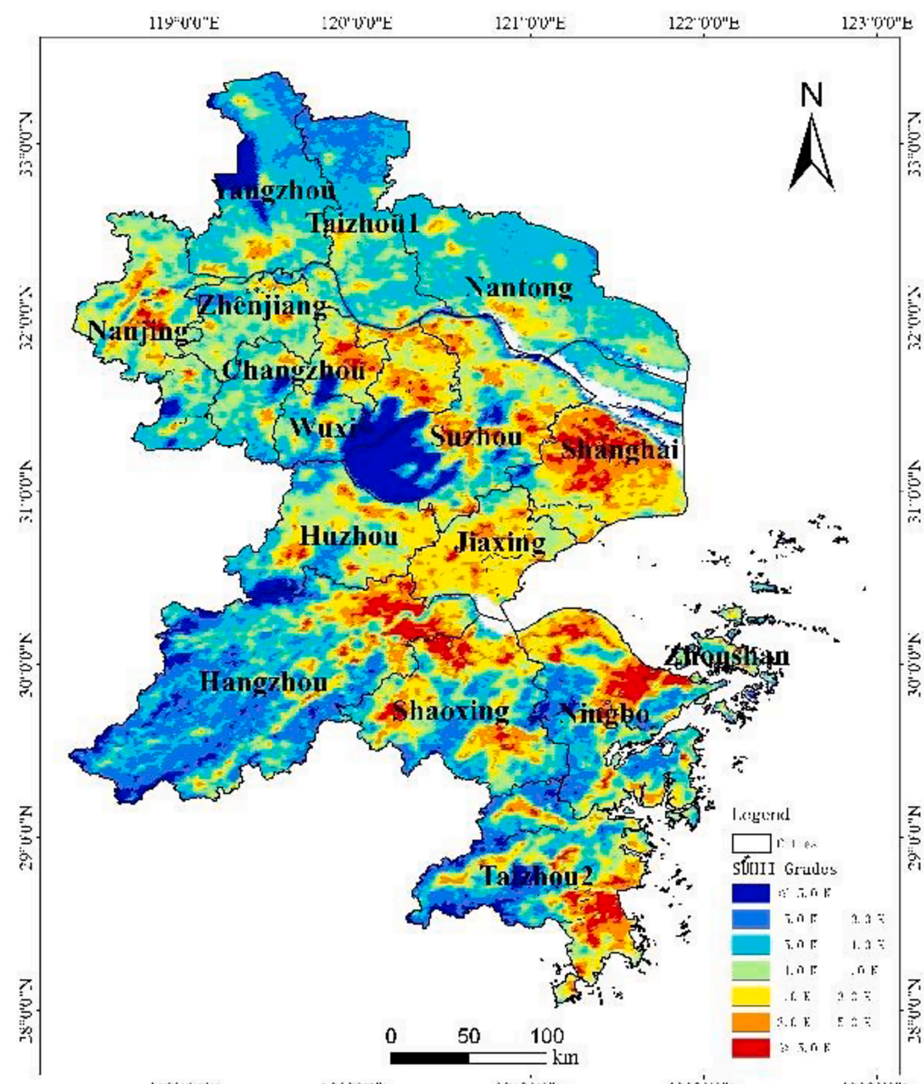

Fig. 2. The Distribution of SUHI intensity in YRDUA in 2015.

agglomeration. As a result, the "SUHI string cluster" centered on Shanghai is growing in coastal areas, including the cities of Hangzhou Bay (e.g., Jiaxing, Hangzhou and Ningbo), while expanding to Nantong, Zhenjiang and Yangzhou, as well as Nanjing in the northwest. Eventually, clusters may form a large regional heat island in a "Z" shape, mimicking the shape of areas affected by urbanization.

3.2. Relationship between SUHI and influencing factors

3.2.1. The contribution of influencing factors

As described in Sect.2.5 multiple factors were selected to evaluate their influence on SUHI. The relative influence of each factor is scaled as a percentage (Carslaw and Taylor, 2009). Fig. 3 presents the results of the BRT analysis for the 16 cities of YRDUA, indicating the relative influence of the natural and anthropogenic factors on SUHI.

Overall, the relative influences of the factors were different in different cities (Fig. 3), as shown by the variability in the vertical direction. On average of most important factors are NTI ISA and NDVI, with 27.62%, 24.38% and 12.11% respectively. NTI has the highest relative influence in Nantong, Shanghai, Shaoxing, Taizhou1, Yangzhou, Zhenjiang and Zhoushan with 35.06%, 32.01%, 33.20%, 43.23%, 39.88%, 25.68% and 29.95% respectively. As regards the other factors, the influencing factors range from high to low are GDP, DEM, POP, BD, WD and RD, with 7.95%, 7.29%, 6.37% and 5.33% respectively on average. The relative influence of natural factors is 48.71%, in which ISA and NDVI are the most influential factors. For anthropogenic factors, the relative influence is 51.29%, in which GDP and POP have a relatively limited influence on SUHI.

The contribution of the influencing factors varies from city to city. In coastal cities for example in Nantong and Jiaxing the contribution rate of natural factors, such as elevation, is relatively low with 1.16% and 5.49% respectively, while the influence of anthropogenic factors, such as POP, is relatively high with 12.49% and 13.77% respectively. For the southern coastal cities, i.e. Ningbo, Taizhou2 and Zhoushan, the situation is reversed, as the contribution rates of elevation are 25.66%, 16.08% and 7.89%, which is relatively high, while the contributions of POP are relatively low, 6.88%, 2.89% and 6.28% respectively. For the cities located along the Yangtze River, such as Nanjing, the influence of NDVI, ISA and NTI is relatively high, with 10.38%, 34.34% and 30.25%, while the influence of DEM, WD and RD is relatively low, with 6.32%, 4.40% and 3.49% respectively. For the cities surrounding the Taihu Lake, such as Changzhou, Wuxi and Suzhou, all factors have approximately the same influence. For business and industrial areas, such as Shanghai, NTI has the largest influence and RD the lowest. In Hangzhou, ISA is the most influential and BD the least.

We selected Hangzhou and Nantong as two case studies to analyze in more detail the influence of each factor on SUHI. As shown in Fig. 4(a), the most influential factor in Hangzhou is ISA, indicating that the urban impervious area is the main cause of SUHI as its relative influence was 41.30% while the lowest one was BD. In Nantong, the NTI is the most influential factor while the DEM is the least.

NDVI influence on SUHI in Hangzhou is high, i.e. rank 4th compared with Nantong, i.e. rank 6th and that is due to the widespread green areas in Hangzhou which help in mitigating SUHI. Among distance-based proximity factors (RD, BD and WD), WD has an obvious influence on SUHI in Nantong, reaching 7.12%, but in Hangzhou, the influence of WD

Cities \ Factors (%)	NTI	ISA	NDVI	GDP	DEM	POP	BD	WD	RD
Changzhou	30.89	38.44	13.07	2.59	1.33	5.09	2.93	3.11	2.55
Hangzhou	18.88	41.30	5.02	2.53	19.63	3.87	2.07	3.15	3.56
Huzhou	13.48	29.85	9.81	12.14	5.68	3.67	9.55	8.36	7.46
Jiaxing	20.96	14.96	22.19	5.98	5.49	13.77	5.60	4.92	6.11
Nanjing	30.25	34.34	10.38	2.72	6.32	4.11	4.02	4.40	3.49
Nantong	35.06	18.16	6.84	9.15	1.16	12.49	6.50	7.12	3.53
Ningbo	24.69	12.99	7.13	8.03	25.66	6.88	5.10	4.43	5.09
Shanghai	32.01	20.44	18.29	9.37	7.61	5.21	3.11	2.07	1.89
Shaoxing	33.20	13.02	31.89	4.84	3.26	2.36	4.33	4.53	2.57
Suzhou	26.01	32.66	7.06	11.87	0.70	2.83	3.97	12.28	2.61
Taizhou1	43.23	20.70	5.32	15.76	2.16	7.92	1.78	1.31	1.82
Taizhou2	15.42	25.36	19.34	5.27	16.08	2.89	7.14	3.50	5.00
Wuxi	22.35	33.65	6.63	7.53	2.32	12.23	4.12	6.26	4.92
Yangzhou	39.88	11.21	12.27	8.62	1.53	7.17	11.33	3.07	4.93
Zhenjiang	25.68	20.65	7.24	10.64	9.89	5.19	8.73	6.22	5.76
Zhoushan	29.95	22.38	11.24	10.11	7.89	6.28	5.03	4.16	2.95

high

low

Fig. 3. The relative influence on SUHI of the selected factors in the 16 cities within the YRD, 2015.

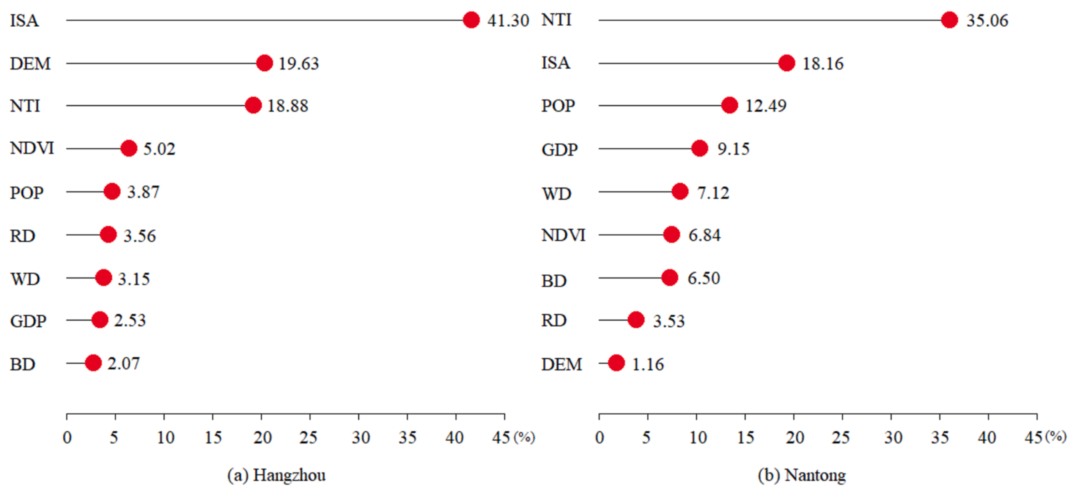

Fig. 4. The relative influence of all factors in 2015. (a) Hangzhou and (b) Nantong.

is not obvious. Besides, it can be concluded that the natural factors have greatest contribution rate on SUHI in Hangzhou. The contribution rates of ISA and DEM accounting 60.93%, while the total contribution of the five anthropogenic factors is 30.91%. Therefore, the natural factors can be more properly used to explain influencing factors in Hangzhou. However, in Shanghai, five anthropogenic factors accounted for 66.73%, which were the main factor affecting SUHI.

3.2.2. *Variation trends of influencing factors*

Overall, each one of the five natural factors, i.e. ISA, NDVI, DEM, WD, LULC, had a comparable influence on SUHI (Fig. 5).

ISA had the highest influence on SUHI of all natural factors, which was expected since a higher ISA indicates lower infiltration and evaporation (Bounoua et al., 2018; Gong et al., 2019). In addition, impervious surfaces tend to have a higher urban surface temperature (Cai et al., 2011; Imhoff et al., 2010). ISA has a lower relative influence on SUHI in the range 0 to 0.25, while the effect increases when ISA > 0.25. When ISA is>0.5, its influence on SUHI is negative but non-negligible. As a kind of man-made material composed of concrete and roads, ISA has the characteristics of rapid heating and cooling, and its thermal characteristics affect the change of surface temperature.

In all cities NDVI is negatively correlated with SUHI (Fig. 5b). In

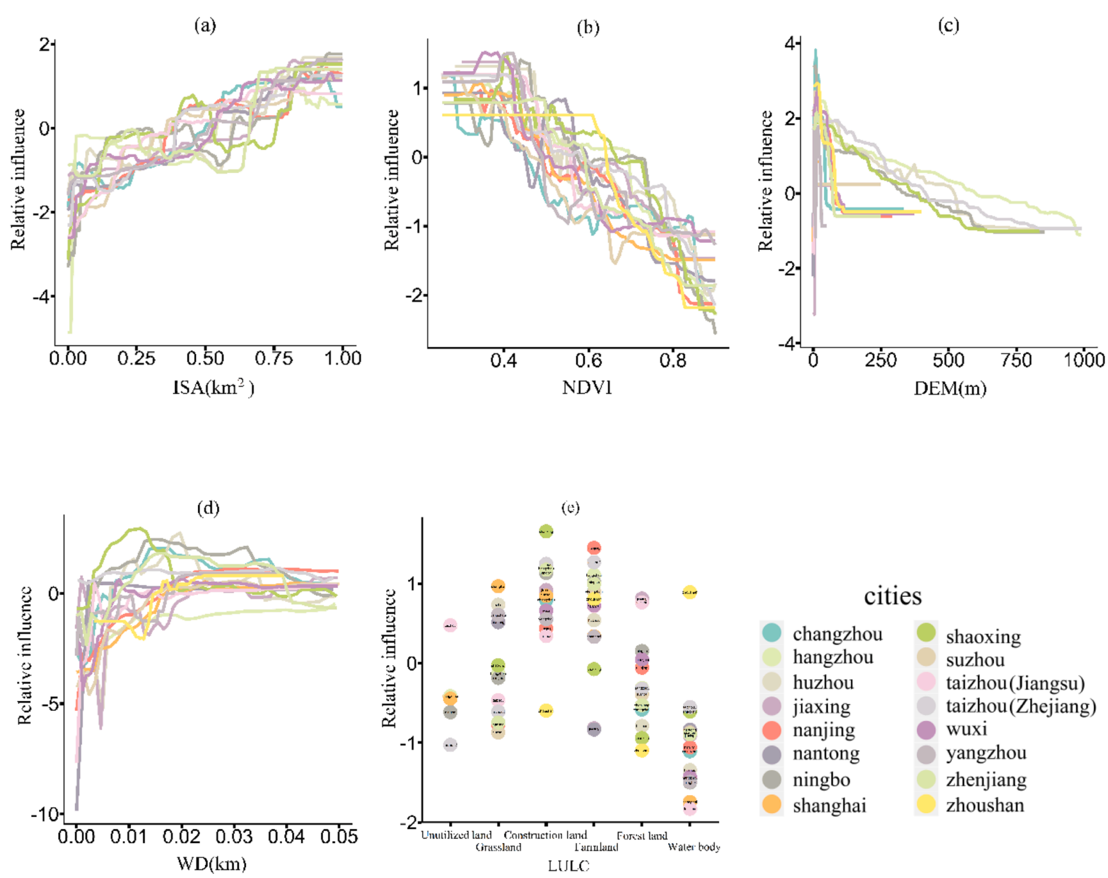

Fig. 5. The influence of natural factors on SUHI: a) ISA, b) NDVI, c) DEM, d) WD and e) LULC; values > 0 indicate a positive influence on SUHI; values < 0 indicate a negative influence on SUHI; values = 0 indicate no influence.

Zhoushan the relative influence of NDVI on SUHI decreases when NDVI > 0.6, indicating that the mitigating effect of vegetation on SUHI is larger at smaller vegetation cover. In Changzhou, when NDVI is in the range (0–0.2), the relative influence on SUHI decreases gradually, then increases before 0.4 and decreases again, reaching the lowest level when NDVI = 0.9. In the other cities, the relative influence shows nonlinear relations with two thresholds. Like Wuxi, there seems to be two thresholds at 0.3 and 0.8. NDVI < 0.3 indicates less vegetation cover than building area, so it has a positive relative influence on SUHI even though fractional abundance of vegetation is small. When NDVI > 0.3, however, the effect of NDVI decreases, reaching its lowest point at 0.85.

As seen in Fig. 5(c), when elevation is in the range (20, 100 m), the relative influence of it on SUHI decreases sharply, while when the value of DEM > 100 m, there is no effect on SUHI. But in Shaoxing, Ningbo, Hangzhou, Huzhou and Taizhou2, when elevation is in the range (0, 600 m), the relative influence on SUHI decreases gradually, then at DEM > 600 m, there is no effect of DEM on SUHI.

When WD is in the range 0–0.02 km (Fig. 5d), the relative influence on SUHI increases, then remains unchanged. In Shaoxing, Changzhou, Ningbo, Huzhou and Zhenjiang, however, when WD increases in the range 0–0.015 km, its relative influence on SUHI increases, then decreases when WD < 0.025 km and finally remains unchanged. These findings confirm that the thermal properties of and the absorption of irradiance by waterbodies do have an influence on the surface temperature of adjacent patches (Wilson et al., 2003) and that this influence extends within a limited range, i.e. 0.25 km.

The impacts of LULC on land surface climate are well documented in literature (Guo et al., 2018; Pramanik and Punia, 2019). We evaluated the relative influences of the unutilized land, grassland, construction land, farmland, forest land and water bodies in the 16 cities (Fig. 5e), which had a documented influence on SUHI in Shaoxing, Nanjing, Shanghai, Jiaxing, Taizhou1 and Zhoushan. The relative influences of LULC on SUHI were in the following order: construction land > farmland > grassland > forest land > unutilized land > water body. The influence of the construction land on SUHI suggests a large influence of human activities. For, the relative influence of farmland in different cities was lower (Fig. 5e), possibly due to the sparse vegetation cover in horticulture farms in the urban areas. Forest land had the lowest influence on SUHI due to the limited extent in urban areas and to the mitigating effect of high transpiration on surface temperature.

As mentioned in Sect.3.2.1, NTI and GDP have the largest influence of all anthropogenic factors, i.e. 27.62% and 7.95% respectively. The relative influence of NTI on SUHI increases rapidly with increasing NTI up to about a value of 1.5, while it was negligible past this value. The relative influence of NTI in most cities is negative in the range (0–1), like Hangzhou, Taizhou1, Ningbo, Zhoushan, Shaoxing. The case of Nantong is slightly different: the relative influence on SUHI increases with increasing the NTI in the range 0–8, the then decreases in the range from 8 to 15, then increases slowly in the range from 15 to 25 up to an asymptotic value.

GDP is the second most important anthropogenic factor. The relative influence of GDP on SUHI increases in the range from 0 to 20000 yuan/km^2, then it remains negligible. In Shanghai, the relative influence of GDP on SUHI was positive, it increased up to 19,000 yuan/km^2, then the effect decreased with GDP in the range 19,000 to 35,000 yuan/km^2. In Nanjing, the relative influence of GDP on SUHI increased up to 30,000 yuan/km^2, then the influence decreased with GDP in the range from 30,000 to 40,000 yuan/km^2, and then it remained constant. In Hangzhou, the relative influence of GDP on SUHI is positive, but it decreased up to 37,000 yuan/km^2, then it remained unchanged. We have applied just two GDP values in our analysis: one value for the rural area and one (higher) value for the urban area for each city. This gives a large improvement in model accuracy at the first split, but no further improvement afterward. This explains the general trend in Fig. 6b.

The total contribution rates of the last three factors, BD, POP and RD are 15.72% (as mentioned in Sect.3.2.1). The relative influence of BD on SUHI decreases with increasing BD in the range of BD up to 0.075 km, and then it remains unchanged. POP is considered an indicator of

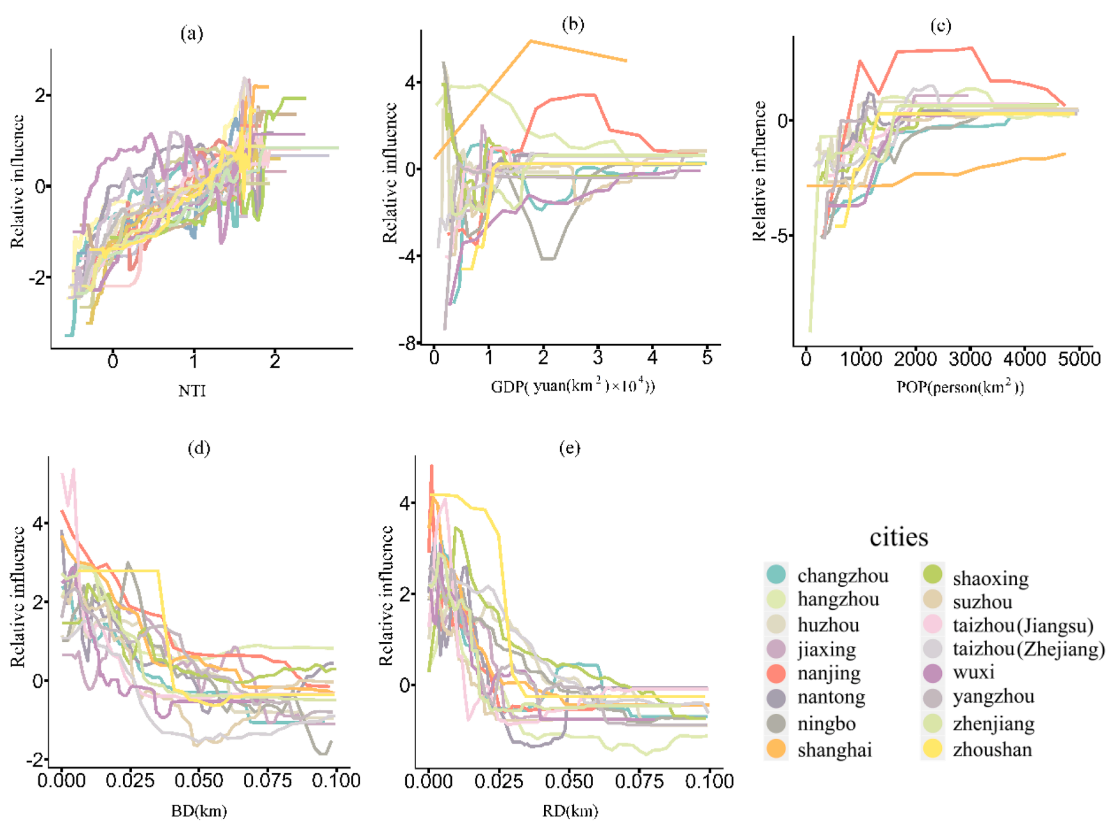

Fig. 6. The influence of anthropogenic factors on SUHI: a) NTI, b) GDP, c) POP, d) BD and e) RD.

anthropogenic heat (Fig. 6c), which reflects the spatial distribution of residents in the way we sampled this data set. The relative influence on SUHI increases up to 2000 person/km^2, then it remains constant and negligible. In Nanjing, the relative influence of POP increases up to 1000 person/km^2. In the range 1000–1500 person/km^2 the relative influence of POP dips a bit, then it increases again and finally levels off to zero. In Shanghai, the relative influence of POP on SUHI is slowly increases. In Ningbo and Nantong, the relative influence of POP increases up to 1000 person/km^2, then decreases slightly in the range 1000–1500 person/km^2 to level off at zero as POP increases further. RD is a measure of urban density: large RD means low urban density. In Nantong, when RD in the range from 0 to 0.035 km, the relative influence on SUHI decreases (Fig. 6e), when RD is from 0.035 to 0.05 km, the relative influence of RD on SUHI increases sharply, then the effect is nihil. In Changzhou, when RD in the range from 0 to 0.035 km, the relative influence of RD on SUHI decreases, when RD is from 0.035 to 0.045 km the relative influence of RD on SUHI increases sharply, then there is steady effect of RD on SUHI, then the relative effect on SUHI again decreased in the range 0.06–0.075 km. For the other cities, the relative influence of RD on SUHI continuously decreases with an increasing RD. When RD is<0.025, its influence on SUHI is positive. From the results, it can be seen that this distance-based proximity factor reflects the radiation effect of the city.

The results are summarized in Table 2 and Table 3.

4. Discussion

The aim of this study was to assess the SUHI dependence on influencing factors in 16 big cities in YRD. Most of high SUHI intensity locations were recorded in cities like Shanghai, Nanjing and Shaoxing, while lower SUHI intensity was recorded in the suburban areas. Impervious surfaces are recoded in the economic and industrial areas that characterize by intensive human activities, SUHI intensity has high values in these areas through changing the percentage of the ISA. Impervious surface is an indicator of human activity intensity and has a great effect on urban surface energy balance (Zhao et al., 2018). Our results show that that the increase in ISA tend to increase SUHI, while an increase in the vegetation cover tends to mitigate the SUHI, confirming the findings of Du et al. (2016), Estoque et al. (2017) Guo et al. (2015), Li et al. (2011), Li et al. (2017) and Yue et al. (2007). ISA and NDVI are highly correlated with SUHI. POP is highly and positively correlated with SUHI effect, especially in rapid urbanization and high income areas and our results agree with Das Majumdar and Biswas (2016).

4.1. Comparison of influential factors with previous studies

This study provides an in-depth quantitative analysis of the causal relationship between influence factors and the SUHI. The idea behind this exercise is that if the change in the influencing factors precedes the change in the SUHI effect, causality is more likely to occur. The results of these analyses show statistically that the SUHI effect is context-dependent, that is, it varies widely in space. Our findings (Figs. 5 and 6) are consistent with those of Buyantuyev and Wu, 2010; Li et al., 2010; Su et al., 2012; Tian et al., 2012. In areas near water bodies (such as Taihu Lake), the situation is reversed by a negative regression coefficient. The results of this study also indicate that SUHI effect is not only influenced by DEM, NVDI, ISA and WD, but also by POP, GDP, NTI, RD and BD. The results show that the increase of DEM, NDVI, RD and BD can significantly reduce the SUHI, while the increase of GDP, NTI, ISA and WD can significantly increase it. We found that DEM, NDVI, ISA, GDP, POP, NTI and RD have a stronger influence on SUHI, which is consistent with Zhang et al. (2017). Air temperature varies between 0.6 and 1.0 K for every 100 m of elevation change. Given its small variations in the study area, the effect of elevation may not be significant.

Policymakers paid less attention to manage SUHI in the YRDUA and more attention to other environmental phenomena, such as traffic

Table 2
Influence of natural factors on SUHI.

Factor	Definition	Relative influence	Reason	Agreement
ISA	ISA is artificial structure that prevents infiltration of water into the soil, includes roofs, paved surfaces (Bounoua et al., 2018; Gong et al., 2019).	The relative influence of ISA on SUHI increasing with increasing ISA in all the 16 selected cities. ISA has a lower relative influence on SUHI in the range 0 to 0.25, while the effect increases when ISA > 0.25. When ISA is>0.5, its influence on SUHI is negative but non-negligible.	As a kind of man-made material composed of concrete and roads, ISA has the characteristics of rapid heating and cooling, and its thermal characteristics affect the change of surface temperature. A higher ISA indicates lower infiltration and evaporation (Bounoua et al., 2018; Gong et al., 2019).	(Chen et al., 2006; Hu et al., 2020a; Yuan and Bauer, 2007).
NDVI	NDVI is normalized difference vegetation index, it reflects vegetation coverage and intensity (Hu et al., 2020b).	**- For Zhoushan:** The relative influence of NDVI on SUHI decreases when NDVI > 0.6, indicating that the mitigating effect of vegetation on SUHI is larger at smaller vegetation cover.**- For Changzhou:** When the value of NDVI is in the range (0–0.2), the relative influence on SUHI decreases gradually, then increases before 0.4 and decrease again, reaching lowest level when NDVI = 0.9.- **For the other cities:** The relative influence shows nonlinear relations with two thresholds. When NDVI less than first threshold, there is a positive relative	This is related to the decrease of surface resistance to evapotranspiration, the majority of energy of latent heat flux and the reduction of Bowen ratio (Mildrexler et al., 2011; Mu et al., 2007).	(Hu et al., 2020b; Yuan and Bauer, 2007)

(*continued on next page*)

Table 2 (*continued*)

Factor	Definition	Relative influence	Reason	Agreement
		influence on SUHI even though fractional abundance of vegetation is small. And then the effect of NDVI decreases, reaching its lowest point at 0.85.		
DEM	DEM is digital elevation model, it characterizes the topographical variation (elevation) of the study area (Wang et al., 2018).	**- For Shaoxing, Ningbo, Hangzhou, Huzhou and Taizhou2:** When DEM (elevation) is in the range (0, 600 m), the relative influence on SUHI decreases gradually, then at DEM > 600 m, there is no effect of DEM on SUHI.- **For the other cities:** When DEM (elevation) is in the range (20, 100 m), the relative influence of it on SUHI decreases sharply, while when the value of DEM > 100 m, there is no effect on SUHI.	Due to orographic effects, SUHI vary with urban-suburban difference in elevation (Zhou et al., 2014a).	(Wang et al., 2018)
WD	WD is one of the distance-based proximity factors, it is the distance from the water (Feng et al., 2019).	**- For Shaoxing, Changzhou, Ningbo, Huzhou, Zhenjiang:** When WD increases in the range 0–0.015 km, its relative influence on SUHI increases, then decreases when WD < 0.025 km and finally remains unchanged.- **For the other cities:** When WD is in the range of 0–0.02 km, the relative influence on SUHI increases, then remains unchanged.	These findings confirm that the thermal properties of and the absorption of irradiance by waterbodies do have an influence on the surface temperature of adjacent patches (Wilson et al., 2003) and that this influence extends within a limited range, i.e. 0.25 km.	(Ghosh and Das, 2018)
LULC	LULC, It has direct relation with the global warming as well as with modification of local climate and environment in a microclimate region (Guo et al., 2018; Pramanik and Punia, 2019).	We evaluated the relative influences of the unutilized land, grassland, construction land, farmland, forest land and water bodies in the 16 cities, which had a documented influence on SUHI in Shaoxing, Nanjing, Shanghai, Jiaxing, Taizhou1 and Zhoushan. The relative influences of LULC on SUHI were in the following order: construction land > farmland > grassland > forest land > unutilized land > water body.	The influence of the construction land on SUHI suggests a large influence of human activities. For, the relative influence of farmland in different cities was lower, possibly due to the sparse vegetation cover in horticulture farms in the urban areas. Forest land had the lowest influence on SUHI due to the limited extent in urban areas and to the mitigating effect of high transpiration on surface temperature.	(Pramanik and Punia, 2019)

congestion and greenhouse gas emissions. Many studies have suggested effective ways for SUHI mitigation. For example, a decrease in the distance from a road is associated with an increase in LST, thus increasing SUHI. To alleviate the latter problem various urban growth management policies, e.g., bus-oriented, compact and corridor development, are being implemented (Adachi et al., 2014; Myint et al., 2015). This points to future research challenges in investigating the effectiveness of urban growth management in reducing the SUHI effect. A smaller WD does help to mitigate SUHI, due to the water thermal properties, consistently with previous studies (Weng et al., 2004; Yue et al., 2007).

4.2. Limitations

This study provided a comprehensive framework to study the relation between SUHI and the influencing factors at different spatial scales in YRDUA. Though, this research has some limitations: Firstly, the study analyzed the spatial patterns of SUHI intensity and the related factor for just the year, 2015). Therefore, this research will continue by applying multi-temporal remote sensing data. Secondly, other influencing factors need also to be studied deeply such as human activities, urban size, and traffic flow. Thirdly, we considered 6 aggregated LULC classes, but a more detailed classification of LULC, for example separating industrial and commercial lands, would be useful to understand better the drivers

Table 3
Influence of anthropogenic factors on SUHI.

Factor	Definition	Relative influence	Reason	Agreement
NTI	NTI is nighttime lighting intensity, it is indicator to the density of human. Low nighttime lighting intensity is directly generated by agricultural activities, especially for undeveloped regions where slow urbanization occurs (Peng et al., 2012).	**- For Nantong:** In the range 0–8, the relative influence on SUHI increases with increasing the NTI, and then decreases in the range from 8 to 15, then increases slowly in the range from 15 to 25 up to an asymptotic value.- **For other cities:** The relative influence of NTI on SUHI increases rapidly with increasing NTI up to about a value of 1.5, while it was negligible past this value. The relative influence of NTI in most cities is negative in the range (0–1), like Hangzhou, Taizhou1, Ningbo, Zhoushan, Shaoxing.	Human activities motivated anthropogenic heat emissions. As a result, at low NTI, i.e. in the transition from rural to low density urban areas increase the temperature difference between urban and suburb (Peng et al., 2012).	(Clinton and Gong, 2013; Liao et al., 2017; Peng et al., 2012; Hu et al., 2020a, p. 32)
GDP	GDP is gross domestic product. It reflect the level of economy in the city (Cui et al., 2016).	**- For Shanghai:**The relative influence of GDP on SUHI was positive, it increased up to 19,000 yuan/km^2, then the effect decreased with GDP in the range 19,000 to 35,000 yuan/km^2.- **For Nanjing:**The relative influence of GDP on SUHI increased up to 30,000 yuan/km^2, then the influence decreased with GDP in the range from 30,000 to 40,000 yuan/km^2, and then it remained constant.- **For Hangzhou:**The relative influence of GDP on SUHI is positive, but it decreased up to 37,000 yuan/km^2, then it remained unchanged.- **For the other cities:**The relative influence of GDP on SUHI increases in the range from 0 to 20000 yuan/km^2, and then it remains negligible.	Sometimes even GDP is high, its relative influences on SUHI is low and this is due to the high protection measures and high green areas to the environment. As in case of Hangzhou, it is the large vegetation areas that are spreading in this city. Hangzhou has given the name of the International Garden City by the International Federation of Park and Recreation.	(Cui et al., 2016; Niu et al., 2020)
BD	BD is one of the distance-based proximity factors, it is the distance from the main building. Large BD means far from building (Feng et al., 2019).	The relative influence of BD on SUHI decreases with increasing BD in the range of BD up to 0.075 km, and then it remains unchanged.	Building is the basic unit of heat generation, whether it is industrial heat source or man-made heat, BD can reflect the radiation effect of the city to a certain extent.	(Schatz and Kucharik, 2015; Zhao et al., 2011; W. Zhou et al., 2014b)
POP	POP is considered an indicators of anthropogenic heat, which reflects the spatial distribution of residents (Du et al., 2016b).	**- For Nanjing:** The relative influence of POP increases up to 1000 person/km^2. In the range 1000–1500 person/km^2 the relative influence of POP dips a bit, then it increases again and finally levels off to zero.- **For Shanghai:**The relative influence of POP on SUHI is slowly increases.- **For Ningbo and Nantong:**The relative influence of POP increases up to 1000 person/km^2, then decreases slightly in the range 1000–1500 person/km^2 to level off at zero as POP increases further.- **For the other Cities:**The relative	This may be related to the measures taken at these cities like increasing the green areas and other measures taken by the residence. Human activities not only can increase the intensity of SUHI, but also can decrease it depending on their behaviors.	(Cui et al., 2016; Du et al., 2016b; Su et al., 2012; Zhang and Wang, 2008)

(*continued on next page*)

Table 3 (*continued*)

Factor	Definition	Relative influence	Reason	Agreement
		influence on SUHI increases up to 2000 person/km^2, then it remains constant and negligible.		
RD	RD it is the distance from main roads to the center. It is a measure of urban density: long RD means low urban density (Feng et al., 2019).	**- For Nantong:** When RD in the range from 0 to 0.035 km, there relative influence on SUHI decreases, when RD is from 0.035 to 0.05 km, the relative influence of RD on SUHI increases sharply, then the effect is nihil.**- For Changzhou:** When RD in the range from 0 to 0.035 km, the relative influence of RD on SUHI decreases, when RD is from 0.03 to 0.045 km, the relative influence of RD on SUHI increases sharply, then there is steady effect of RD on SUHI, then the relative effect on SUHI again decreased in the range 0.06–0.075 km.**- For the other Cities:** The relative influence of RD on SUHI continuously decreases with an increasing RD. When RD is<0.025, its influence on SUHI is positive.	As a kind of man-made material composed of concrete, roads have the characteristics of rapid heating and cooling, and its thermal characteristics affect the change of surface temperature.	(Feng et al., 2019)

of urban climate. Fourthly, urban areas have different design in different regions, which makes it more complex to study influence factors. Therefore, further studies are needed to address this aspect. Finally, the limitation of the low spatial resolution remote sensing imagery used in this study should be overcome by using higher resolution remote sensing images to extract urban land-cover information.

This study analyzed the spatial variability of SUHI effect for a heterogeneous region and selecting multiple influencing variables. Our study differs from previous studies in three aspects. First, previous studies focused on one or two influencing factors, while we selected a comprehensive set of natural and anthropogenic factors. Second, previous studies focused on direct influencing factors, while this study focused on direct and indirect influences by calculating the distance from buildings, the major road and water. Third, our study provided further analysis of the influence factors and SUHI in each selected city, such as how to fully understand the relationships between POP, NDVI and SUHI and how to apply these results in urban management and planning. Future work will include the application of time series analysis to study the temporal variability of SUHI and the contribution of the influencing factors. This study will help us better understand the effect natural and anthropogenic factors on SUHI and help decision makers to develop more sustainable urban environments.

5. Conclusions

This paper took YRDUA, a major urban agglomeration in Eastern China, as a case study and made quantitative analyses to investigate the influence of multiple factors on SUHI intensity in 2015. MODIS data were used in this study. The spatial pattern of SUHI intensity was differently distributed, as it was most severe in the center and southeast. Three main conclusions can be summarized. Firstly, NTI and ISA are the two most influential factors on SUHI, while RD variations have a smaller influence. The total contribution of anthropogenic factors (NTI, GDP, POP, BD, RD) was 51.29% and natural factors (ISA, NDVI, WD, DEM) was 48.71%, indicating that SUHI is highly affected by anthropogenic factors. The order of influence of LULC on SUHI are as follows: construction land > farmland > grassland > forest land > unutilized land > water body. Secondly, in this study, both NTI and NDVI are significantly correlated with the SUHI intensity. Comparatively, GDP and RD have a non-significant correlation with SUHI. Thirdly, the variation in the socioeconomic level lead to different spatial patterns of different influence factors.

In summary, the influence of NTI and ISA on SUHI is higher in each city, while the influence is lower in case of RD. It has been also detected that the overall mean SUHI intensity is affected by the development of the city. Distance-based proximity factors (like RD and BD) are negatively correlated SUHI, while ISA and POP are positively correlated. So we recommend that these factors should be considered in cities future urban planning. The findings from this study might be relevant for urban planning within a framework to control SUHI.

CRediT authorship contribution statement

Zian Wang: Conceptualization, Methodology, Software, Writing - original draft. **Qingyan Meng:** Supervision. **Mona Allam:** Visualization. **Die Hu:** Formal analysis. **Linlin Zhang:** Software. **Massimo Menenti:** Writing - review & editing.

Declaration of Competing Interest

The authors declare that they have no known competing financial interests or personal relationships that could have appeared to influence the work reported in this paper.

Acknowledgment

This work was supported by Hainan Major Science and Technology Project [ZDKJ2019006], and the Major Projects of High-Resolution Earth Observation Systems of National Science and Technology [05-Y30B01-9001-19/20-1] and the MOST High Level Foreign Expert program (Grant nr. G20190161018).

References

Adachi, S.A., Kimura, F., Kusaka, H., Duda, M.G., Yamagata, Y., Seya, H., Nakamichi, K., Aoyagi, T., 2014. Moderation of summertime heat island phenomena via

modification of the urban form in the Tokyo metropolitan area. J. Appl. Meteorol. Climatol. 53, 1886–1900. https://doi.org/10.1175/JAMC-D-13-0194.1.
Ayanlade, A., 2016. Seasonality in the daytime and night-time intensity of land surface temperature in a tropical city area. Sci. Total Environ. 557–558, 415–424. https://doi.org/10.1016/j.scitotenv.2016.03.027.
Bennett, M.M., Smith, L.C., 2017. Advances in using multitemporal night-time lights satellite imagery to detect, estimate, and monitor socioeconomic dynamics. Remote Sens. Environ. 176–197. https://doi.org/10.1016/j.rse.2017.01.005.
Bounoua, L., Nigro, J., Zhang, P., Thome, K., Lachir, A., 2018. Mapping urbanization in the United States from 2001 to 2011. Appl. Geogr. 90, 123–133. https://doi.org/10.1016/j.apgeog.2017.12.002.
Buyantuyev, A., Wu, J., 2010. Urban heat islands and landscape heterogeneity: linking spatiotemporal variations in surface temperatures to land-cover and socioeconomic patterns. Landscape Ecol. 25, 17–33. https://doi.org/10.1007/s10980-009-9402-4.
Cai, G., Du, M., Xue, Y., 2011. Monitoring of urban heat island effect in Beijing combining ASTER and TM data. Int. J. Remote Sens. 32, 1213–1232. https://doi.org/10.1080/01431160903469079.
Carslaw, D.C., Taylor, P.J., 2009. Analysis of air pollution data at a mixed source location using boosted regression trees. Atmos. Environ. 43, 3563–3570. https://doi.org/10.1016/j.atmosenv.2009.04.001.
Chen, X.-L., Zhao, H.-M., Li, P.-X., Yin, Z.-Y., 2006. Remote sensing image-based analysis of the relationship between urban heat island and land use/cover changes. Remote Sens. Environ. Therm. Remote Sens. Urban Areas 104, 133–146. https://doi.org/10.1016/j.rse.2005.11.016.
Chen, Z., Yu, B., Hu, Y., Huang, C., Shi, K., Wu, J., 2015. Estimating house vacancy rate in metropolitan areas using NPP-VIIRS nighttime light composite data. IEEE J. Sel. Top. Appl. Earth Observations Remote Sens. 8, 2188–2197. https://doi.org/10.1109/JSTARS.2015.2418201.
Clinton, N., Gong, P., 2013. MODIS detected surface urban heat islands and sinks: Global locations and controls. Remote Sens. Environ. 134, 294–304.
Coseo, P., Larsen, L., 2014. How factors of land use/land cover, building configuration, and adjacent heat sources and sinks explain Urban Heat Islands in Chicago. Landcape Urban Plan. 125, 117–129. https://doi.org/10.1016/j.landurbplan.2014.02.019.
Cui, Y., Liu, J., Hu, Y., Wang, J., Kuang, W., 2012. Modeling the radiation balance of different urban underlying surfaces 57, 1046–1054.
Cui, Y., Xu, X., Dong, J., Qin, Y., 2016. Influence of urbanization factors on surface urban heat island intensity: a comparison of countries at different developmental phases. Sustainability 8, 706. https://doi.org/10.3390/su8080706.
Das Majumdar, D., Biswas, A., 2016. Quantifying land surface temperature change from LISA clusters: an alternative approach to identifying urban land use transformation. Landscape Urban Plann. 153, 51–65. https://doi.org/10.1016/j.landurbplan.2016.05.001.
Deilami, K., Kamruzzaman, Md., Liu, Y., 2018. Urban heat island effect: a systematic review of spatio-temporal factors, data, methods, and mitigation measures. Int. J. Appl. Earth Obs. Geoinf. 67, 30–42. https://doi.org/10.1016/j.jag.2017.12.009.
Du, H., Song, X., Jiang, H., et al., 2016. Research on the cooling island effects of water body: A case study of Shanghai, China. Ecol. Indic. 67, 31–38. https://doi.org/10.1016/j.ecolind.2016.02.040.
Du, H., Song, X., Jiang, H., Kan, Z., Wang, Z., Cai, Y., 2016a. Research on the cooling island effects of water body: a case study of Shanghai, China. Ecol. Ind. 67, 31–38. https://doi.org/10.1016/j.ecolind.2016.02.040.
Du, H., Wang, D., Wang, Y., Zhao, X., Qin, F., Jiang, H., Cai, Y., 2016b. Influences of land cover types, meteorological conditions, anthropogenic heat and urban area on surface urban heat island in the Yangtze River Delta Urban Agglomeration. Sci. Total Environ. 571, 461–470. https://doi.org/10.1016/j.scitotenv.2016.07.012.
Du, S., Xiong, Z., Wang, Y.-C., Guo, L., 2016c. Quantifying the multilevel effects of landscape composition and configuration on land surface temperature. Remote Sens. Environ. 178, 84–92. https://doi.org/10.1016/j.rse.2016.02.063.
Elvidge, C.D., Baugh, K.E., Kihn, E.A., Kroehl, H.W., Davis, E.R., Davis, C.W., 1997. Relation between satellite observed visible-near infrared emissions, population, economic activity and electric power consumption. Int. J. Remote Sens. 18, 1373–1379. https://doi.org/10.1080/014311697218485.
Estoque, R.C., Murayama, Y., Myint, S.W., 2017. Effects of landscape composition and pattern on land surface temperature: an urban heat island study in the megacities of Southeast Asia. Sci. Total Environ. 577, 349–359. https://doi.org/10.1016/j.scitotenv.2016.10.195.
Feng, Y., Gao, C., Tong, X., Chen, S., Lei, Z., Wang, J., 2019. Spatial patterns of land surface temperature and their influencing factors: a case study in Suzhou, China. Remote Sens. 11, 182. https://doi.org/10.3390/rs11020182.
Friedman, J.H., 2002. Stochastic gradient boosting. Comput. Stat. Data Anal. 38 (4), 367–378. https://doi.org/10.1016/S0167-9473(01)00065-2.
Gao, J., Yu, Z., Wang, L., Vejre, H., 2019. Suitability of regional development based on ecosystem service benefits and losses: a case study of the Yangtze River Delta urban agglomeration, China. Ecol. Indicat. 107, 105579 https://doi.org/10.1016/j.ecolind.2019.105579.
Ghosh, S., Das, A., 2018. Modelling urban cooling island impact of green space and water bodies on surface urban heat island in a continuously developing urban area. Model. Earth Syst. Environ. 4, 501–515. https://doi.org/10.1007/s40808-018-0456-7.
Gong, P., Li, X., Zhang, W., 2019. 40-Year (1978–2017) human settlement changes in China reflected by impervious surfaces from satellite remote sensing. Sci. Bull. 64, 756–763. https://doi.org/10.1016/j.scib.2019.04.024.
Gu, C., 2011. Climate change and urbanization in the Yangtze River Delta. Habitat International 9.
Guo, F., Lenoir, J., Bonebrake, T.C., 2018. Land-use change interacts with climate to determine elevational species redistribution. Nat. Commun. 9, 1315. https://doi.org/10.1038/s41467-018-03786-9.
Guo, G., Wu, Z., Xiao, R., Chen, Y., Liu, X., Zhang, X., 2015. Impacts of urban biophysical composition on land surface temperature in urban heat island clusters. Landscape Urban Plann. 135, 1–10. https://doi.org/10.1016/j.landurbplan.2014.11.007.
Hien, W.N., Kardinal Jusuf, S., Samsudin, R., Eliza, A., Ignatius, M., 2011. A climatic responsive urban planning model for high density city: Singapore's commercial district. Int. J. Sustain. Build. Technol. Urban Dev. 2, 323–330. https://doi.org/10.5390/SUSB.2011.2.4.323.
Hu, D., Meng, Q., Zhang, L., Zhang, Y., 2020a. Spatial quantitative analysis of the potential driving factors of land surface temperature in different "Centers" of polycentric cities: a case study in Tianjin, China. Sci. Total Environ. 706, 135244 https://doi.org/10.1016/j.scitotenv.2019.135244.
Hu, Y., Ban, Y., Zhang, Q., Liu, J., et al., 2009. The trajectory of urbanization process in the Yangtze River delta during 1990 to 2005. 2009 Joint Urban Remote Sensing Event 1–8. https://doi.org/10.1109/URS.2009.5137536.
Hu, Y., Dai, Z., Guldmann, J.-M., 2020b. Modeling the impact of 2D/3D urban indicators on the urban heat island over different seasons: a boosted regression tree approach. J. Environ. Manage. 266, 110424 https://doi.org/10.1016/j.jenvman.2020.110424.
Huang, G., Cadenasso, M.L., 2016. People, landscape, and urban heat island: dynamics among neighborhood social conditions, land cover and surface temperatures. Landscape Ecol. 31, 2507–2515. https://doi.org/10.1007/s10980-016-0437-z.
Huang, Q., Lu, Y., 2015. The effect of urban heat island on climate warming in the yangtze river delta urban agglomeration in China. IJERPH 12, 8773–8789. https://doi.org/10.3390/ijerph120808773.
Imhoff, M.L., Zhang, P., Wolfe, R.E., Bounoua, L., 2010. Remote sensing of the urban heat island effect across biomes in the continental USA. Remote Sens. Environ. 114, 504–513. https://doi.org/10.1016/j.rse.2009.10.008.
Jusuf, S.K., Wong, N.H., Hagen, E., Anggoro, R., Hong, Y., 2007. The influence of land use on the urban heat island in Singapore. Habitat Int. 31, 232–242. https://doi.org/10.1016/j.habitatint.2007.02.006.
Kotharkar, R., Surawar, M., 2016. Land use, land cover, and population density impact on the formation of canopy urban heat islands through traverse survey in the Nagpur urban area, India. J. Urban Plann. Dev. 142, 04015003. https://doi.org/10.1061/(ASCE)UP.1943-5444.0000277.
Li, J., Song, C., Cao, L., Zhu, F., Meng, X., Wu, J., 2011. Impacts of landscape structure on surface urban heat islands: a case study of Shanghai, China. Remote Sens. Environ. 115, 3249–3263. https://doi.org/10.1016/j.rse.2011.07.008.
Li, L., Huang, X., Li, J., Wen, D., 2017a. Quantifying the spatiotemporal trends of Canopy Layer Heat Island (CLHI) and its driving factors over wuhan, china with satellite remote sensing. Remote Sens. 9, 536. https://doi.org/10.3390/rs9060536.
Li, S., Zhao, Z., Miaomiao, X., Wang, Y., 2010. Investigating spatial non-stationary and scale-dependent relationships between urban surface temperature and environmental factors using geographically weighted regression. Environ. Modell. Softw. 25, 1789–1800. https://doi.org/10.1016/j.envsoft.2010.06.011.
Li, X., Zhou, Y., Asrar, G.R., Imhoff, M., Li, Xuecao, 2017b. The surface urban heat island response to urban expansion: a panel analysis for the conterminous United States. Sci. Total Environ. 605–606, 426–435. https://doi.org/10.1016/j.scitotenv.2017.06.229.
Liao, W., Liu, X., Wang, D., Sheng, Y., 2017. The impact of energy consumption on the surface Urban Heat Island in China's 32 Major Cities. Remote Sens. 9, 250. https://doi.org/10.3390/rs9030250.
Liu, L., Zhang, Y., 2011. Urban heat island analysis using the Landsat TM data and ASTER data: a case study in Hong Kong. Remote Sens. 3, 1535–1552. https://doi.org/10.3390/rs3071535.
Liu, Y., Fang, X., Xu, Y., Zhang, S., Luan, Q., 2018. Assessment of surface urban heat island across China's three main urban agglomerations. Theor. Appl. Climatol. 133, 473–488. https://doi.org/10.1007/s00704-017-2197-3.
Liu, Y., Wu, C., Peng, D., Xu, S., Gonsamo, A., Jassal, R.S., Altaf Arain, M., Lu, L., Fang, B., Chen, J.M., 2016. Improved modeling of land surface phenology using MODIS land surface reflectance and temperature at evergreen needleleaf forests of central North America. Remote Sens. Environ. 176, 152–162. https://doi.org/10.1016/j.rse.2016.01.021.
Lo, C.P., Quattrochi, D.A., Luvall, J.C., 1997. Application of high-resolution thermal infrared remote sensing and GIS to assess the urban heat island effect. Int. J. Remote Sens. 18, 287–304. https://doi.org/10.1080/014311697219079.
Lu, D., Li, G., Kuang, W., Moran, E., 2014. Methods to extract impervious surface areas from satellite images. Int. J. Digital Earth 7, 93–112. https://doi.org/10.1080/17538947.2013.866173.
Martilli, A., Roth, M., Chow, W.T.L., Demuzere, M., Lipson, M., Krayenhoff, E.S., Sailor, D., Nazarian, N., Voogt, J., Wouters, H., Middel, A., Stewart, I.D., Bechtel, B., Christen, A., Hart, M.A., 2020. Summer average urban-rural surface temperature differences do not indicate the need for urban heat reduction (preprint). Open Sci. Framework. https://doi.org/10.31219/osf.io/8gnbf.
Mildrexler, D.J., Zhao, M., Running, S.W., 2011. A global comparison between station air temperatures and MODIS land surface temperatures reveals the cooling role of forests. J. Geophys. Res. 116, G03025. https://doi.org/10.1029/2010JG001486.
Mu, Q., Heinsch, F.A., Zhao, M., Running, S.W., 2007. Development of a global evapotranspiration algorithm based on MODIS and global meteorology data. Remote Sens. Environ. 111, 519–536. https://doi.org/10.1016/j.rse.2007.04.015.
Myint, S.W., Zheng, B., Talen, E., Fan, C., Kaplan, S., Middel, A., Smith, M., Huang, H., Brazel, A., 2015. Does the spatial arrangement of urban landscape matter? examples of urban warming and cooling in phoenix and las vegas. Ecosyst. Health Sustainability 1, 1–15. https://doi.org/10.1890/EHS14-0028.1.

Nguyen, T.D., Shih, M.-H., Srivastava, D., Tirthapura, S., Xu, B., 2019. Stratified Random Sampling from Streaming and Stored Data 12.

Niu, L., Tang, R., Jiang, Y., Zhou, X., 2020. Spatiotemporal patterns and drivers of the surface Urban Heat Island in 36 major cities in China: a comparison of two different methods for delineating rural areas. Sustainability 12, 478. https://doi.org/10.3390/su12020478.

Oke, T.R., 1995. The Heat Island of the Urban Boundary Layer: Characteristics, Causes and Effects, in: Cermak, J.E., Davenport, A.G., Plate, E.J., Viegas, D.X. (Eds.), Wind Climate in Cities. Springer Netherlands, Dordrecht, pp. 81–107. https://doi.org/10.1007/978-94-017-3686-2_5.

Oke, T.R., 1982. The energetic basis of the urban heat island. Q. J. R. Meteorolog. Soc. 108, 1–24. https://doi.org/10.1002/qj.49710845502.

Oke, T.R., 1973. City size and the urban heat island. Atmosph. Environ. Pergamon Press 769–779.

Peng, S., Piao, S., Ciais, P., Friedlingstein, P., Ottle, C., Bréon, F.-M., Nan, H., Zhou, L., Myneni, R.B., 2012. Surface Urban Heat Island Across 419 Global Big Cities. Environ. Sci. Technol. 46, 696–703. https://doi.org/10.1021/es2030438.

Pramanik, S., Punia, M., 2019. Land use/land cover change and surface urban heat island intensity: source–sink landscape-based study in Delhi. India. Environ. Dev. Sustain. https://doi.org/10.1007/s10668-019-00515-0.

R Development Core Team, 2006. R: A Language and Environment for Statistical Computing. R Foundation for Statistical Computing.

Schatz, J., Kucharik, C.J., 2015. Urban climate effects on extreme temperatures in Madison, Wisconsin, USA. Environ. Res. Lett. 10, 094024 https://doi.org/10.1088/1748-9326/10/9/094024.

Schwarz, N., Lautenbach, S., Seppelt, R., 2011. Exploring indicators for quantifying surface urban heat islands of European cities with MODIS land surface temperatures. Remote Sens. Environ. 115, 3175–3186. https://doi.org/10.1016/j.rse.2011.07.003.

Seto, K.C., Reenberg, A., Boone, C.G., Fragkias, M., Haase, D., Langanke, T., Marcotullio, P., Munroe, D.K., Olah, B., Simon, D., 2012. Urban land teleconnections and sustainability. Proc. Natl. Acad. Sci. 109, 7687–7692. https://doi.org/10.1073/pnas.1117622109.

Shi, K., Yu, B., Huang, Y., et al., 2014. Evaluating the Ability of NPP-VIIRS Nighttime Light Data to Estimate the Gross Domestic Product and the Electric Power Consumption of China at Multiple Scales: A Comparison with DMSP-OLS Data. Remote Sens. 6 (2), 1705–1724. https://doi.org/10.3390/rs6021705.

Sobrino, J.A., Jimenez-Munoz, J.C., Soria, G., Romaguera, M., Guanter, L., Moreno, J., Plaza, A., Martinez, P., 2008. Land surface emissivity retrieval from different VNIR and TIR sensors. IEEE Trans. Geosci. Remote Sensing 46, 316–327. https://doi.org/10.1109/TGRS.2007.904834.

Stankowski, S.J., 1972. Population Density as an Indirect Indicator of Urban and Suburban Land-Surface Modifications.

Streutker, D.R., 2003. Satellite-measured growth of the urban heat island of Houston, Texas. Remote Sens. Environ. 85, 282–289. https://doi.org/10.1016/S0034-4257(03)00007-5.

Su, Y.-F., Foody, G.M., Cheng, K.-S., 2012. Spatial non-stationarity in the relationships between land cover and surface temperature in an urban heat island and its impacts on thermally sensitive populations. Landscape Urban Plann. 107, 172–180. https://doi.org/10.1016/j.landurbplan.2012.05.016.

Sun, Y., Gao, C., Li, J., Wang, R., Liu, J., 2019. Evaluating urban heat island intensity and its associated determinants of towns and cities continuum in the Yangtze River Delta Urban Agglomerations. Sustainable Cities and Society 50, 101659. https://doi.org/10.1016/j.scs.2019.101659.

Tan, M., Li, X., 2015. Quantifying the effects of settlement size on urban heat islands in fairly uniform geographic areas. Habitat Int. 49, 100–106. https://doi.org/10.1016/j.habitatint.2015.05.013.

Tian, F., Qiu, G.Y., Yang, Y.H., Xiong, Y.J., Wang, P., 2012. Studies on the relationships between land surface temperature and environmental factors in an inland river catchment based on geographically weighted regression and MODIS data. IEEE J Sel. Top. Appl. Earth Observ. Remote Sens. 5, 687–698. https://doi.org/10.1109/JSTARS.2012.2190978.

Tian, G., 2011. The urban growth, size distribution and spatio-temporal dynamic pattern of the Yangtze River Delta megalopolitan region, China. Ecol. Model. 14.

United Nations, 2014. World Urbanization Prospects: The 2013 Revision.

Tucker, C.J., Vanpraet, C.L., Sharman, M.J., et al., 1985. Satellite remote sensing of total herbaceous biomass production in the senegalese sahel: 1980–1984. Remote Sens. Environ. 17 (3), 223–249.

Wan, Z., 2008. New refinements and validation of the MODIS land-surface temperature/emissivity products. Remote Sens. Environ. 112, 59–74. https://doi.org/10.1016/j.rse.2006.06.026.

Wang, Y., Bakker, F., de Groot, R., Wörtche, H., 2014. Effect of ecosystem services provided by urban green infrastructure on indoor environment: a literature review. Build. Environ. 77, 88–100. https://doi.org/10.1016/j.buildenv.2014.03.021.

Wang, Y., Du, H., Xu, Y., Lu, D., Wang, X., Guo, Z., 2018. Temporal and spatial variation relationship and influence factors on surface urban heat island and ozone pollution in the Yangtze River Delta, China. Sci. Total Environ. 631–632, 921–933. https://doi.org/10.1016/j.scitotenv.2018.03.050.

Weng, Q., 2009. Thermal infrared remote sensing for urban climate and environmental studies: Methods, applications, and trends. ISPRS J. Photogramm. Remote Sens. 64, 335–344. https://doi.org/10.1016/j.isprsjprs.2009.03.007.

Weng, Q., Liu, H., Liang, B., Lu, D., 2008. The Spatial variations of urban land surface temperatures: pertinent factors, zoning effect, and seasonal variability. IEEE J. Sel. Top. Appl. Earth Observ. Remote Sens. 1, 154–166. https://doi.org/10.1109/JSTARS.2008.917869.

Weng, Q., Lu, D., Schubring, J., 2004. Estimation of land surface temperature–vegetation abundance relationship for urban heat island studies. Remote Sens. Environ. 89, 467–483. https://doi.org/10.1016/j.rse.2003.11.005.

Wilson, J.S., Clay, M., Martin, E., Stuckey, D., Vedder-Risch, K., 2003. Evaluating environmental influences of zoning in urban ecosystems with remote sensing. Remote Sens. Environ. 86, 303–321. https://doi.org/10.1016/S0034-4257(03)00084-1.

Yang, X., Hou, Y., Chen, B., 2011. Observed surface warming induced by urbanization in east China. J. Geophys. Res. 116, 263–294. https://doi.org/10.1029/2010jd015452.

Yang, X., Leung, L.R., Zhao, N., et al., 2017. Contribution of urbanization to the increase of extreme heat events in an urban agglomeration in east China. Geophys. Res. Lett. 6940–6950. https://doi.org/10.1002/2017GL074084.

Yu, B., Tang, M., Wu, Q., et al., 2018. Urban Built-Up Area Extraction From Log-Transformed NPP-VIIRS Nighttime Light Composite Data. IEEE Geosci. Remote Sens. Lett. 15 (8), 1279–1283. https://doi.org/10.1109/LGRS.2018.2830797.

Yuan, F., Bauer, M.E., 2007. Comparison of impervious surface area and normalized difference vegetation index as indicators of surface urban heat island effects in Landsat imagery. Remote Sens. Environ. 106, 375–386. https://doi.org/10.1016/j.rse.2006.09.003.

Yue, W., Xu, J., Tan, W., Xu, L., 2007. The relationship between land surface temperature and NDVI with remote sensing: application to Shanghai Landsat 7 ETM+ data. Int. J. Remote Sens. 28, 3205–3226. https://doi.org/10.1080/01431160500306906.

Zhang, H., Qi, Z., Ye, X., Cai, Y., Ma, W., Chen, M., 2013. Analysis of land use/land cover change, population shift, and their effects on spatiotemporal patterns of urban heat islands in metropolitan Shanghai, China. Appl. Geogr. 44, 121–133. https://doi.org/10.1016/j.apgeog.2013.07.021.

Zhang, J., Wang, Y., 2008. Study of the relationships between the spatial extent of surface urban heat islands and urban characteristic factors based on Landsat ETM+ Data. Sensors 8, 7453–7468. https://doi.org/10.3390/s8117453.

Zhang, Liqiang, Liu, W., Hou, K., Lin, J., Song, C., Zhou, C., Huang, B., Tong, X., Wang, J., Rhine, W., Jiao, Y., Wang, Ziwei, Ni, R., Liu, M., Zhang, Liang, Wang, Ziye, Wang, Yuebin, Li, X., Liu, S., Wang, Yanhong, 2019. Air pollution exposure associates with increased risk of neonatal jaundice. Nat. Commun. 10, 3741. https://doi.org/10.1038/s41467-019-11387-3.

Zhang, X., Estoque, R.C., Murayama, Y., 2017. An urban heat island study in Nanchang City, China based on land surface temperature and social-ecological variables. Sustain. Cities Soc. 32, 557–568. https://doi.org/10.1016/j.scs.2017.05.005.

Zhao, C., Fu, G., Liu, X., Fu, F., 2011. Urban planning indicators, morphology and climate indicators: a case study for a north-south transect of Beijing, China. Build. Environ. 46, 1174–1183. https://doi.org/10.1016/j.buildenv.2010.12.009.

Zhao, H., Ren, Z., Tan, J., 2018. The spatial patterns of land surface temperature and its impact factors: spatial non-stationarity and scale effects based on a geographically-weighted regression model. Sustainability 10, 2242. https://doi.org/10.3390/su10072242.

Zhao, M., Cai, H., Qiao, Z., Xu, X., 2016. Influence of urban expansion on the urban heat island effect in Shanghai. Int. J. Geograph. Inform. Sci. 30, 2421–2441. https://doi.org/10.1080/13658816.2016.1178389.

Zhou, D., Bonafoni, S., Zhang, L., Wang, R., 2018. Remote sensing of the urban heat island effect in a highly populated urban agglomeration area in East China. Sci. Total Environ. 628–629, 415–429. https://doi.org/10.1016/j.scitotenv.2018.02.074.

Zhou, D., Zhao, S., Liu, S., Zhang, L., Zhu, C., 2014a. Surface urban heat island in China's 32 major cities: spatial patterns and drivers. Remote Sens. Environ. 152, 51–61. https://doi.org/10.1016/j.rse.2014.05.017.

Zhou, W., Qian, Y., Li, X., Li, W., Han, L., 2014b. Relationships between land cover and the surface urban heat island: seasonal variability and effects of spatial and thematic resolution of land cover data on predicting land surface temperatures. Landscape Ecol. 15.

Zhou, W., Qian, Y., Li, X., Li, W., Han, L., 2014c. Relationships between land cover and the surface urban heat island: seasonal variability and effects of spatial and thematic resolution of land cover data on predicting land surface temperatures. Landscape Ecol. 29, 153–167. https://doi.org/10.1007/s10980-013-9950-5.